IJE TRANSACTIONS A: Basics Vol. 37 No. 07, (July 2024) 1343-1356

International Journal of Engineering

Journal Homepage: www.ije.ir

Analysis of Nucleation Time of Gas Hydrates in Presence of Paraffin During Mechanized Oil Production

G. Y. Korobov, A. A. Vorontsov*, G. V. Buslaev, V. T. Nguyen

Petroleum Engineering Department, Empress Catherine II Saint Petersburg Mining University, Saint Petersburg, Russia

P A P E R I N F O

Paper history:
Received 19 December 2023
Received in revised form 21 February 2024
Accepted 07 March 2024

Keywords:
Gas Hydrates
Asphalt-resin-paraffin Deposits
Waxes
Gas Hydrate Formation Time
Kinetic Inhibitor of Hydrate Formation

A B S T R A C T

The objective of this study is to investigate the nucleation timing of gas hydrate molecules in oil flows. This research focuses on examining how paraffin particles impact the formation timing of hydrate deposits during the mechanical production of oil. A thorough comprehension and control over the formation of organic deposits within the wellbore can substantially mitigate equipment maintenance expenses, enhance the safety and consistency of production, and bolster the economic viability of extracting hydrocarbons. The initial segment of the paper outlines a methodology for identifying the formation depths of gas hydrates and asphaltene-resin-paraffin deposits (ARPD) in operational oil wells through the resolution of thermobaric differential equation systems. Subsequent laboratory experiments were conducted to assess the nucleation timing of gas hydrates in the presence of paraffin. These tests were performed in a specialized high-pressure autoclave that enables the establishment of requisite thermobaric conditions. An internal agitator in the autoclave facilitates the needed dispersion within the system to emulate well flow conditions. Experimental findings revealed that paraffin particles impede the formation of gas hydrate deposits and decelerate their nucleation process. Notably, a 3% increase in paraffin concentration within the mixture was observed to prolong the nucleation timing of gas hydrates by a factor of nine. Based on the review of available literature, it is deduced that further comprehensive investigations are essential for the advancement of a temporal model governing the operational dynamics of production wells under the influence of gas hydrate and ARPD formation.

***doi**: 10.5829/ije.2024.37.07a.13*

[1]

Graphical Abstract

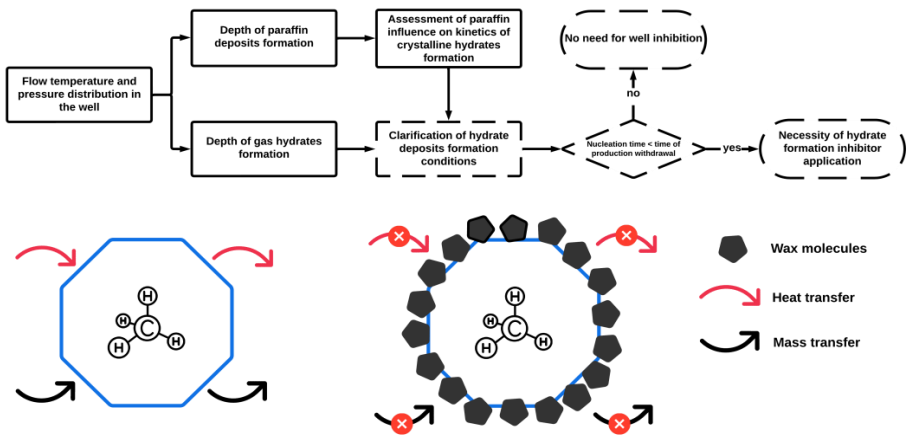

Disturbance of mass and heat exchange between hydrates due to wax particles

*Corresponding Author Email: *andrey-vorontsov98@yandex.ru* (A.A. Vorontsov)

Please cite this article as: Korobov GY, Vorontsov AA, Buslaev GV, Nguyen VT. Analysis of Nucleation Time of Gas Hydrates in Presence of Paraffin During Mechanized Oil Production. International Journal of Engineering, Transactions A: Basics. 2024;37(07):1343-56.

1. INTRODUCTION

Gas hydrates, also known as clathrates, are crystalline structures where water molecules form a lattice that encases gas molecules under specific temperature and pressure conditions. The thermodynamic prerequisites for gas hydrate formation vary according to gas type, temperature, pressure, gas saturation, and the salinity of water (1) as well as the compositional makeup of other phases present. Methane (CH_4), ethane (C_2H_6), propane (C_3H_8), butane (C_4H_{10}), carbon dioxide (CO_2), hydrogen sulfide (H_2S), nitrogen (N_2), and other gases in hydrocarbon production can form hydrates under suitable conditions (2). Methane-based natural gas hydrates are particularly notable for their energy potential, with one cubic meter of hydrate yielding approximately 165 standard cubic meters of CH_4.

The formation of gas hydrates can be classified into anthropogenic and natural occurrences. Anthropogenic hydrates may develop in oil and natural gas production systems characterized by a high gas-to-oil ratio, including areas such as the bottom hole zone, wellbores, and field pipelines (3). In contrast, natural hydrates may aggregate into clusters or exist in a dispersed state (4). The genesis of anthropogenic natural gas hydrates poses considerable challenges to the operational efficiency of oil and gas production facilities by complicating technological processes, escalating energy demands, shortening equipment maintenance intervals, and amplifying risks in the exploration of new Arctic oil and gas ventures (5, 6).

The formation of asphaltene-resin-paraffin deposits (ARPD) in oilfield equipment is a more prevalent issue than gas hydrate deposition. The development of numerous fields in the Volga-Ural and West Siberian oil and gas provinces is hindered by ARPD formation (7).

The severe climatic conditions of the Far North, exacerbated by permafrost cooling of flows, coupled with the rigorous climate, amplify the challenges associated with gas hydrate and ARPD formation during oil and gas extraction (8, 9). The coalescence of gas hydrates and ARPD into a unified deposit further complicates the operation of production wells. Therefore, refining the theoretical understanding of gas hydrate and ARPD formation is crucial for the enhanced exploitation of Arctic territories within the Russian Federation (10, 11).

For the most part, it is imperative to acknowledge that the thermobaric conditions prevailing within a well exert a profound influence on the process of hydrocarbon production process. The pressure and temperature parameters of the flow within the well are critical determinants in the formation of organic deposits (12). In this context, a methodology for assessing the flow temperature inside the borehole was introduced by researchers (13). This approach is grounded in differential equations of heat conduction, incorporating the heat transfer coefficient between the surrounding rock formations and the well's flow. The determination of this coefficient leverages field-derived data (14). The phenomenon of convective heat transfer in vertical gas-liquid two-phase hydrocarbon flows has been examined (15, 16), with laboratory experiments revealing the relationship between the heat transfer and the velocity and structure of the mixture. The theoretical endeavors have culminated in the formulation of an elaborate mechanistic model for heat transfer. This model accounts for the flow's pattern, distinguishing among bubble, slug, and annular structures, and is adept at predicting the flow structure before calculating the flow's hydrodynamics and heat transfer characteristics based on the anticipated structure. The results of comparison between the model and real data showed that presented model calculates the heat transfer coefficient with an error margin of 20%, 30%, and 25% for bubble, annular, and slug flows, respectively. Furthermore, the integration of permafrost attributes such as the latent heat of fusion (17), alongside considerations of permafrost thawing, the migration of water from proximal zones around the well to more remote areas, and the temperature gradient, has facilitated the introduction of a novel thermal model for a producing well by the authors (18). Field tests of the model showed high convergence of the calculation results with real data.

Additionally, the impact of operating an electrical submersible pump (ESP) on the heat exchange dynamics between the pumped fluid and its surroundings warrants attention. Investigations (14, 19) have delved into the thermal interactions between an active ESP unit and its immediate environment, proposing a model that accurately predicts the temperature variations of both the unit itself and the fluid in transit through and around the pump. Moreover, the processes of well killing and the injection of specialized fluids can induce cooling in the bottom hole zone and wellbore, potentially leading to the augmented formation of ARPD and gas hydrates within the well space. This phenomenon poses challenges to the subsequent reactivation and operation of the well (20, 21).

Research documented in studies (22, 23) has highlighted the considerable impact of flow dynamics on hydrate formation, specifically through mechanisms such as destruction, coalescence, and deformation of gas bubbles, as well as their interactions with mixture flow vortices and collisions among themselves. Further investigation (24) elucidated the nuances of hydrate formation across varying levels of water content within the flow, yielding the following insights:

1. High water content facilitates hydrate nucleation at the gas-water phase boundary, significantly accelerating the agglomeration process of gas hydrates.
2. At medium water content, hydrate nucleation predominantly occurs at the oil-water interface, resulting

in fewer hydrate deposits and a reduced rate of hydrate formation.

3. Systems with low water content exhibit decreased density and thickness in gas hydrate deposits.

These findings underscore the critical importance of understanding hydrate formation dynamics under various well conditions.

Hydrate deposit management commonly employs the use of hydrate formation inhibitors (25), which are categorized by most researchers based on literature (26):

- Their mechanism of action, dividing them into thermodynamic, kinetic, and anti-agglomerant types.
- Composition, distinguishing between single-component and multi-component inhibitors.
- The number and nature of functions they perform.
- Physical and chemical properties, such as density, volatility, and freezing point.

The accumulation of asphalt-resin-paraffin deposits (ARPD) on field equipment and pipeline surfaces poses significant challenges to oil production, transportation, and refining processes (27). Key factors contributing to ARPD formation in field equipment have been identified (28) as:

- The presence of heavy oil components that agglomerate into large ARPD particles.
- The release of oil-dissolved gases when flow pressure falls below the gas saturation pressure of oil.
- Reduction of flow temperature beneath the paraffin saturation point of oil.
- Situations where disruptive flow forces, dependent on velocity, regime, and structure, are outweighed by the cohesive forces within the deposits.

The most effective technological approach for ARPD management involves the use of chemical inhibitors with a crucial focus on minimizing inhibitor loss (29) due to adsorption by the surrounding rock formations (30). A comprehensive methodology for mitigating ARPD formation in the wellbore area has been proposed (31), incorporating well washing with specialized solvents to dissolve existing deposits. Additionally, other strategies for combating ARPD formation in production wells have been explored (32). Investigations (33-35) have examined how the material composition of production pipes influences ARPD formation conditions. Another study (36) introduced a heating cable system as a method for controlling paraffin deposition in production wells, while research (37) presented a novel approach involving magnetic reagent treatment of oilfield equipment.

As previously discussed, the concurrent formation of gas hydrates and asphalt-resin-paraffin deposits (ARPD) significantly complicates hydrocarbon productions via mechanized methods (38, 39). Research presented by Wang et al. (40) introduced an advanced model for hydrate nucleation in the presence of ARPD and surfactants, with asphaltenes potentially acting as such surfactants, as illustrated in Figure 1. The study yielded several key findings:

1. The nucleation process of hydrate molecules is decelerated by the presence of ARPD or surfactants.
2. ARPD molecules obstruct the mass and heat transfer process between hydrate molecules.
3. The volume of hydrate deposits escalates in the absence of surfactants but in the presence of ARPD. This increase is attributed to the integration of ARPD molecules into the hydrate agglomerates, further complicating their disintegration.

Therefore, the primary aim of this research is to delve into the dynamics of gas hydrate deposit formation within a producing well, particularly in scenarios where oil flow contains wax particles. Laboratory observations could facilitate the development of a temporal model for a producing well. This model enables the prediction of the time required for product removal and the formation of organic deposits. Under certain conditions, this model suggests that gas hydrates may not accumulate in bottom hole equipment to a significant extent. Consequently, this allows for a strategic adjustment in the delivery of hydrate formation inhibitors to surface equipment rather than directly to the bottom hole. Such a shift in the inhibitor delivery strategy is anticipated to streamline equipment maintenance and substantially reduce the financial burden associated with the injection of reagents into the wellbore.

2. METHODOLOGY

2. 1. Methodology for Determining Depth of Gas Hydrate and ARPD Formation in a Well The methodology for identifying the initial depths of organic deposits formation is structured around a comprehensive algorithm that encompasses several critical steps:

1. Initial Setup: Define the initial well configuration and production conditions based on field data to establish a baseline for further analysis.

2. ESP Operating Parameters: Determine the operational parameters of the Electrical Submersible Pump (ESP) unit, incorporating adjustments for emulsions and free gas content to ensure accurate modeling of the pump's performance under field conditions.

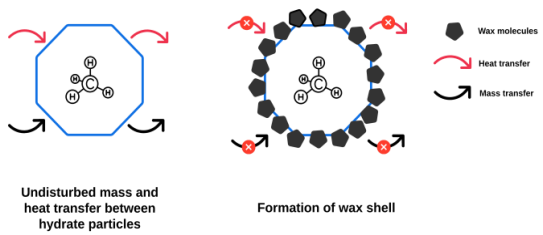

Figure 1. Disturbance of mass and heat exchange between hydrates due to wax particles

3. Temperature Distribution Evaluation: Assess the temperature distribution along the well's depth, taking into account the heat generated by the ESP unit (38). This step is crucial for understanding the thermal dynamics within the wellbore.

4. Pressure Distribution Calculation: Utilize the updated Poetman-Carpenter method to calculate the pressure distribution at various depths within the well for both the production string and tubing. This method provides a refined approach to estimating pressure profiles.

5. Linking Pressure to Temperature: Correlate the depth-specific pressure values with corresponding flow temperature readings. This correlation specifies the P(T) distribution within the well, offering a detailed view of the thermobaric conditions.

6. Well Operation Modeling: Estimate the true operational parameters of the well under the specified conditions using a well operation model. This step involves specifying the flow rate, bottom hole pressure, and receiving pressure, thereby refining the operational parameters.

7. Hydrate Formation Equilibrium: Compare the P(T) distribution against the equilibrium conditions for hydrate formation to identify the onset depth of hydrate formation (22). This comparison is vital for pinpointing where hydrates begin to form within the well.

8. Thermogram and Wax Crystallization: Match the well's thermogram against the temperature profile for wax crystallization across the well's depth to determine the formation depth of paraffin.

A block diagram illustrating this algorithm is depicted in Figure 2; providing a visual representation of the process flow.

Upon implementing this algorithm, it is possible to achieve accurate determination of the initial depths for ARPD and crystalline hydrate formation. To further enhance this algorithm, incorporating a time variable into the calculations can account for the kinetics of gas hydrate formation in the presence of ARPD, making the model more dynamic and reflective of real-world conditions (41, 42).

For the initial determination of organic deposits formation depths, the pressure characteristic of the ESP

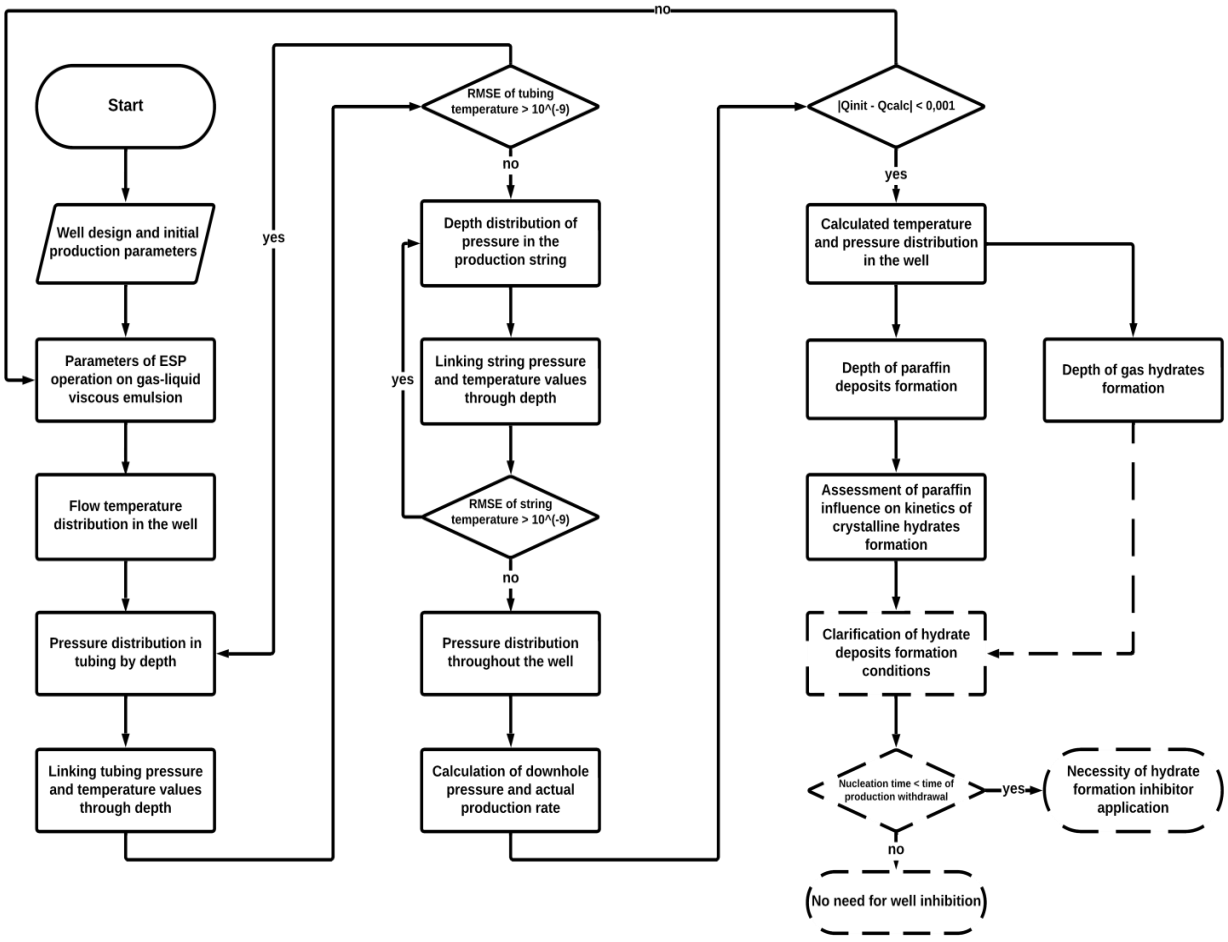

Figure 2. Algorithm to determine the depth of organic sediment formation

in emulsion with gas presence is established. The pump's pressure output is derived from its passport characteristics, which are then recalibrated for a viscous liquid using Lyapkov method (43). This recalibration involves determining the pump stage's coefficient of rapidity, denoted as n_s, as outlined in Equation 1:

$$n_s = 193 \cdot n \cdot \left(\frac{Q_{liq.optim.}}{86400}\right)^{0,5} \cdot \left(g \cdot \frac{H_{liq.optim.}}{z}\right)^{-0,75} \quad (1)$$

where n is the number of pump revolutions, rpm; $Q_{liq.optim.}$, $H_{liq.optim.}$ - optimum flow rate (m^3/day) and pump head on water (m); z - number of stages.

Reynolds number of the flow in the channels of ESP, Equation 2:

$$Re_H = \frac{4,3+0,816 \cdot {n_s}^{0,274}}{{n_s}^{0,575}} \cdot \frac{Q_{liq}}{\left(\frac{\mu_{mix}}{\rho_{mix}}\right) \cdot 86400} \cdot \sqrt[3]{\frac{n \cdot 86400}{Q_{liq.optim.}}} \quad (2)$$

where μ_{mix}, ρ_{mix} are mixture viscosity ($Pa \cdot s$) and density (kg/m^3); Q_{liq} - well flow rate, m^3/day.

Conversion factors for viscous fluid, Equations 3 and 4:

$$K_{HQ} = 1 - \left(3,585 - 0,821 \cdot lg(Re_H)\right) \cdot \left(0,027 + 0,0485 \frac{Q_{liq.}}{Q_{liq.optim.}}\right) \quad (3)$$

$$K_\eta = \begin{cases} 0,485 \cdot lg(Re_H) - 0,63 - 0,26 \frac{Q_{liq}}{Q_{liq.optim.}} \; if \; Re_H < 2320 \\ 0,274 \cdot lg(Re_H) - 0,06 - 0,14 \frac{Q_{liq}}{Q_{liq.optim.}} \; if \; Re_H > 2320 \end{cases} \quad (4)$$

Coefficients for recalculation of the water-air mixture are now calculated using the corresponding nomogram in Figure 3 (44).

The gas content is found by Equation 5:

$$\Gamma = G \Big/ \left(\frac{\rho_{oil.degas}}{\rho_{gas}} + G\right) \quad (5)$$

where G - gas factor, m^3 /m^3; $\rho_{oil.degas}$ - density of degassed oil at standard conditions, kg/m^3; ρ_{gas} – density of gas at standard conditions, kg/m^3.

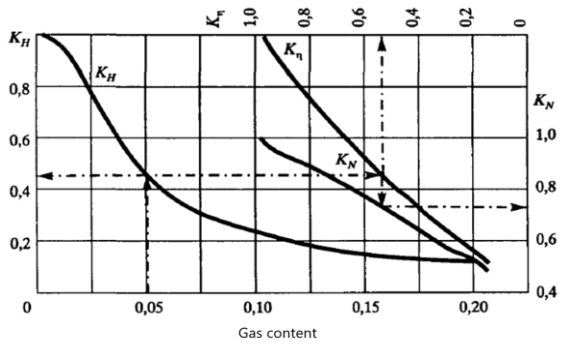

Figure 3. Nomogram for calculating pump performance parameters for water-air mixtures (44)

To accurately calculate the pressure produced by the pump P_{pump} for any given well flow rate, the approach involves obtaining conversion factors for gas. These factors are then multiplied by the coefficients determined for viscous fluids, enabling the characterization of the pump's performance with the actual emulsion present in the well. This step is crucial for understanding the pump's ability to maintain optimal pressure levels under various operational conditions, thereby ensuring the efficient transport of the fluid mixture to the surface.

The flow temperature in any section between the reservoir roof and the pump (temperature in the production string) is determined with Equation 6, the flow temperature in any section of the tubing is determined with Equation 7:

$$T_{str} = T_{res} - (H_{res} - H) \cdot cos\alpha \cdot \frac{0,0034+0,79 \cdot Grad \cdot cos\alpha}{10^{Q_{liq}/86400 \cdot 20 \cdot d^{2,67}_{str.inner}}} \quad (6)$$

$$T_{tub} = T_{res} - \left(H_{res} - H_p\right) \cdot cos\alpha \cdot \frac{0,0034 + 0,79 \cdot Grad \cdot cos\alpha}{10^{Q_{liq}/86400 \cdot 20 \cdot d^{2,67}_{str.inner}}} - \left(H_p - H\right) \cdot cos\alpha \cdot \frac{0,0034 + 0,79 \cdot \Gamma \cdot cos\alpha}{10^{Q_{liq}/86400 \cdot 20 \cdot d^{2,67}_{tub.inner}}} + \Delta t_{pump} \quad (7)$$

where α is the average well inclination angle; *Grad* is the temperature gradient, grad/m; H_p - vertical depth of pump suspension, m; T_{res} - reservoir temperature, °C; H_{res} - vertical depth of the reservoir roof, m; $d_{str.inner}$ - inner diameter of production string, m; $d_{tub.inner}$ - inner diameter of tubing, m. The temperature distribution along the borehole is shown in Figure 4.

Temperature rise at the pump outlet (45) is determined with Equation 8:

$$\Delta t_{pump} = \frac{g H_{pump}}{c} \left(\frac{1}{\eta_{pump} \eta_{motor}} - \frac{0,5}{\eta_{pump}}\right) \quad (8)$$

where H_{pump} – is the head created by the pump, m; η_{pump} - pump efficiency, shares; η_{motor} - motor efficiency equal to 0.9.

A modernized Poetman-Carpenter methodology can be used to determine the pressure distribution in the well. Modernization includes modified equations to account

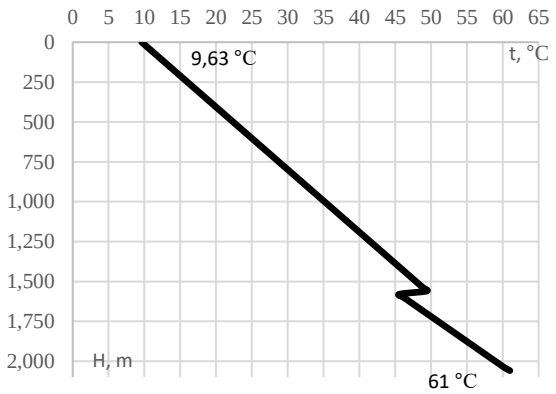

Figure 4. Flow temperature distribution along the borehole

for separated and dissolved gas in the tubing string after the ESP unit. The separation factor of the pump, which is used for modernization, is determined with Equation 9:

$$Ksep = \frac{1}{\left(1+0{,}75\cdot\frac{Q_{liq}}{86400\cdot(0.02\cdot\left(\pi\frac{\left(d_{str.inner}^2-d_{pump}^2\right)}{4}\right)}\right)} \quad (9)$$

The Poetman-Carpenter methodology is used to find the pressure gradient in the well, Equation 10:

$$\frac{dP}{dH} = \rho_{mix}\cdot 9{,}81\cdot 10^{-6} * cos\alpha + \frac{\left[f\cdot Q^2\cdot(1-\beta_{water})^2\cdot {M_{mix}}^2\right]}{\left(2{,}3\cdot 10^{15}\cdot\rho_{mix}\cdot {d_{tub.inner}}^5\right)} \quad (10)$$

where ρ_{mix} is mixture density, kg/m^3; β_{water} - water cut, shares; M_{mix} - specific density of the gas-liquid mixture, kg/m^3. These parameters are found according to the Poetman-Carpenter methodology.

Calculations are executed in a "top-down" manner within the tubing to the point of saturation pressure, and similarly, within the production string, extending from the pump inlet pressure to the bottomhole pressure (39). By employing the iterative method (46) key operational parameters of the well can be determined. Through numerical integration, we ascertain the pressure distribution along the tubing. Initially, pressures at designated depths are computed via a mathematical interpolation technique, subsequently linking these pressures with new temperature values. This process involves multiple iterations to accurately determine the pressure distribution throughout the depth of both the tubing and production string, culminating in the precise calculation of the true bottom hole pressure, P_{bot}. The derived pressure distribution along the wellbore is depicted in Figure 5.

Then, through a well productivity coefficient K_{prod}, the true flow rate of the well is found. Vogel correction (47), in Equation 11, is also introduced in the calculations which takes into account the movement of aerated liquid flow.

$$Q = \begin{cases} K_{prod}\cdot(P_{res}-P_{bot}),\ if\ P_{bot} > P_{sat} \\ K_{prod}\cdot(P_{res}-P_{bot}) + \frac{K_{prod}\cdot P_{sat}}{1{,}8}\cdot \\ \cdot\left(1-0{,}2\cdot\frac{P_{bot}}{P_{sat}}-0{,}8\cdot\left(\frac{P_{bot}}{P_{sat}}\right)^2\right),\ if\ P_{bot}\le P_{sat} \end{cases} \quad (11)$$

The calculated flow rate value is reintegrated at the beginning of the calculation, and the entire algorithm is iterated until the desired precision is achieved. Subsequently, the equilibrium conditions for the formation of crystalline hydrates are established utilizing the calculation methodologies shown in the referenced monographs (48, 49). These methodologies are specifically tailored for application to both natural and associated petroleum gases.

First, using Equation 12, the pressure of gas hydrate formation p_m^0 (in MPa) is calculated (p_m^0 is determined for temperature T_0 =273.15 K). Equation 12 is applicable for hydrates of cubic structure II, which, in turn, are typical for oil and gas condensate fields, which are considered in this paper.

$$\left[1+p_m^0\left(2{,}5y_{CH_4}+1{,}4y_{CO_2}+0{,}67y_{N_2}+46{,}1y_{H_2S}\right)\right]^2 = \frac{1}{p_m^0\left(\frac{y_{CH_4}}{231}+\frac{y_{C_2H_6}}{2{,}3}+\frac{y_{C_3H_8}}{0{,}176}+\frac{y_{i-C_4H_{10}}}{0{,}113}+\frac{y_{n-C_4H_{10}}}{1{,}6}+\frac{y_{CO_2}}{26{,}3}+\frac{y_{N_2}}{2323}+\frac{y_{H_2S}}{10{,}47}\right)} \quad (12)$$

where y is the mole fraction of each component of the gas mixture. The content of each component in the gas is also determined after field studies or according to field development guidelines.

The desired pressure (p_m) at temperatures higher than 273.15 K is found using sets of reference curves of hydrate formation proposed by Semenov et al. (50) by the following Equation 13.

$$p_m = \frac{p_m^0 z^0}{z} exp\left(A_1\left(\frac{1}{T_0}-\frac{1}{T}\right)\right) \quad (13)$$

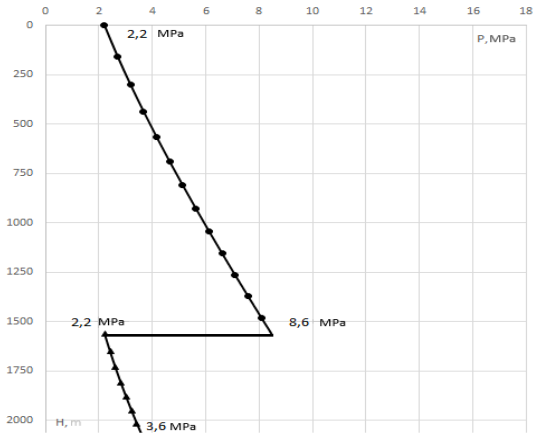

Figure 5. Pressure distribution along the wellbore obtained with modernized Poetman-Carpenter method

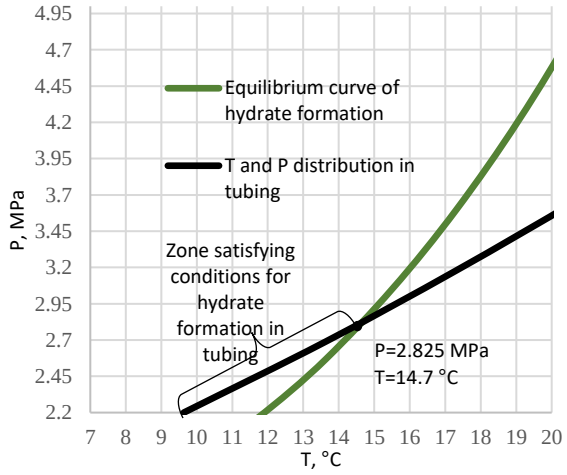

Figure 6. Determination of hydrate formation interval in tubing

z^0, z are gas compressibility coefficient for p_m^0 and T_0 conditions and calculated conditions, respectively; A_1 - empirical coefficient (50).

Employing this methodology yields an equilibrium condition curve for hydrate formation plotted in pressure-temperature (P-T) coordinates, as illustrated in Figure 6. The point where this curve intersects with another indicates the initial depth at which gas hydrate begins to form within the tubing.

To calculate the depth of ARPD formation in the well, it is necessary to find the wax crystallization temperature distribution (51). The values of pressure and volume gas content are taken from previously calculated Poetman-Carpenter method. The dependence of paraffin crystallization temperature on depth is presented in Equation 14:

$$T_{wax}(P_i) = t_0 + 0{,}2\ P_i - 0{,}1\ V_{gas.sat,i} \quad (14)$$

where t_0 is found by Equation 15 (°C); P_i and $V_{gas.sat,i}$ - borehole section pressure (MPa) and residual gas saturation of oil (m^3/m^3), determined with the Poetman-Carpenter methodology.

$$t_0 = 11{,}398 + 34{,}084\ lgC_{wax} \quad (15)$$

where C_{wax} - mass content of paraffin, %.

The outcomes of this research are depicted in Figure 7. The algorithm introduced is slated for enhancement through the incorporation of supplementary differential equations. These equations aim to ascertain the duration required for the formation of organic deposits within the borehole space, as well as the extraction time for the fluid lifted from the borehole to the wellhead.

This advancement seeks to refine the predictive accuracy of the algorithm, providing a more comprehensive understanding of the dynamics involved in the deposition and extraction processes within the well operation.

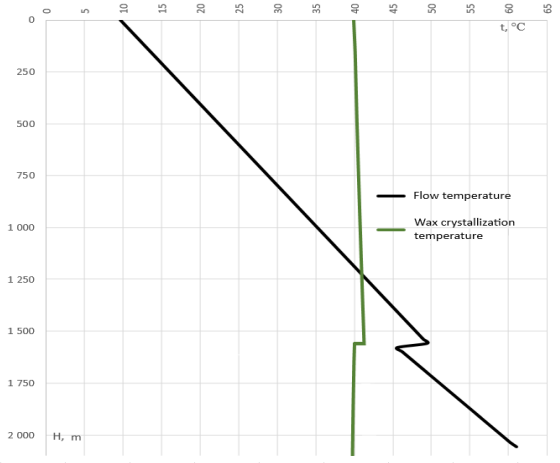

Figure 7. Determining the depth of ARPD formation in the well

2. 2. Methodology for Determining Thermobaric Conditions of Gas Hydrates Formation in Presence of Paraffin

The concurrent formation of crystalline hydrates and waxes poses a substantial challenge to oil production infrastructure. The accumulation of gas hydrate and wax deposits within pipelines and wells can significantly diminish productivity and, in severe cases, entirely obstruct the flow of liquids (27, 41, 52). Therefore, investigating this phenomenon is crucial for devising effective strategies for the prevention of deposit formation and for the efficient removal of such deposits during the operational lifecycle of oil fields.

In this section, we delve into the methodology employed in laboratory experiments designed to evaluate the impact of wax on gas hydrate formation conditions. By varying the mass content of dissolved paraffin, it is feasible to delineate the correlation between the conditions of gas hydrate formation and the quantity of paraffin present in the system. The experiments were conducted using the specialized reactor-autoclave Gas Hydrate Autoclave GHA 350 and a model gas preparation system, enabling the investigation of hydrate formation at temperatures ranging from -10°C to 60°C and pressures up to 35 MPa, as depicted in Figure 8. This research methodology was meticulously developed and validated by the personnel of the Scientific Center "Arctic" at the Empress Catherine II Saint Petersburg Mining University.

The laboratory experiment methodology, inspired by the approach detailed by Semenov et al. (53), is outlined as follows:

1. **Preparation of Paraffin Solution in Kerosene:**

- Aviation kerosene TS-1 (GOST 10227-86) with paraffin P-2 (GOST 23683-89) dissolved in it serves as the simulated hydrocarbon medium.
- Initially, 125 ml of the kerosene solution containing paraffin and 200 ml of water are utilized to

Figure 8. Laboratory complex for gas hydrate research: A. Autoclave GHA-350; B. Top-driven stirrer; C. Huber Ministat 240 thermostat; D. Gas boosters with maximum pressures of 40.0 MPa (left) and 15.0 MPa (right); E. Model gas preparation system.

create a phase interface within the camera lens. The mass for 125 ml of kerosene is accurately measured, considering the container's mass, yielding 96.71 g of kerosene. Following the measurement of the requisite volume, the container is sealed to prevent the vaporization of kerosene.

- The necessary quantity of paraffin is determined based on its desired mass content in the kerosene, ranging from 2-10% wt. The precise amount of paraffin wax is calculated using the appropriate proportion.
- The paraffin is then integrated into the pre-measured kerosene, followed by thorough mixing. To ensure containment, containers with screw-on lids, specifically designed for reagents, are employed to maintain airtight conditions upon heating.
- To expedite the dissolution of paraffin wax in kerosene, the container is placed within an oven preheated to temperatures of 50-60°C. This heating facilitates the complete dissolution of paraffin into kerosene within 30 minutes.

2. Autoclave Preparation for the Experiment:

- The autoclave's internal cavity is meticulously cleaned of residues from prior experiments using a solvent followed by alcohol, ensuring a contaminant-free environment for the new experiment.
- It is then loaded with 125 ml of kerosene solution and 200 ml of water. This specific ratio is crucial for visibly distinguishing phase separation in the first camera and gas-liquid interaction in the second camera.
- The experiment's requisite pressure is established, initially set to 40 bar for the commencement of the experiment.
- To generate the necessary emulsion, the solution is agitated at room temperature at a speed of 800 rpm for a duration of 30 minutes, rendering the autoclave primed for experimentation.

3. Conducting the Experiment to Identify the Equilibrium Point of Hydrate Formation:

- The system is pressurized with methane to slightly above the required pressure to ensure that, following methane dissolution and system equilibration, the pressure remains at or above the experiment's threshold. In this instance, the system is pressurized to 45 bar before stabilizing at 40 bar.
- The agitator's speed is adjusted to a moderate 100-200 rpm, facilitating the saturation of the liquid with methane.
- The system is then cooled to a temperature below the anticipated hydrate formation threshold. Maintaining the system in a super cooled state for a period allows for equilibrium establishment without the risk of hydrate formation due to oversaturation, as the stirrer operates at low speeds.
- To induce gas hydrate formation, the agitator speed is increased to 500 rpm, establishing a turbulent regime within the autoclave. In these oversaturated and super cooled conditions, hydrate crystals form abruptly throughout the autoclave volume, marked by a significant pressure drop and a minor temperature increase—indicative of the exothermic nature of hydrate formation. Additionally, a noticeable increase in stirrer torque occurs as the forming hydrate crystals impede the agitation process.
- Identifying the equilibrium point involves gradual heating of the system at a constant rate. The equilibrium conditions for hydrate formation and dissociation align, but the stochastic nature of hydrate formation complicates direct equilibrium point determination during cooling. During dissociation, the equilibrium point is discerned at the pressure curve's inflection point. As the system is slowly heated, hydrate crystals disintegrate, releasing gas and elevating autoclave pressure. Once hydrate decomposition is complete, the pressure curve stabilizes, rising more gradually as pressure increases are solely attributed to heating. The experiment maintains a heating rate of 1°C every two hours, facilitating precise equilibrium point determination. To chart the equilibrium curve for hydrate formation, equilibrium points across various thermobaric conditions are identified.

2. 3. Methodology for Studying the Nucleation Time of Gas Hydrates in Presence of Paraffin

During laboratory studies on hydrate formation in the presence of paraffin, it was discovered that under conditions of low system pressures and low temperatures, the hydrate nucleation time significantly increases. This observation led to the conclusion that paraffin particles play a role in affecting the kinetics of the gas hydrate crystal formation process. Specifically, due to the pronounced super cooling at the lower pressures where hydrate formation occurs, paraffin particles tend to precipitate first within the liquid's volume. These particles, therefore, interfere with mass and heat transfer processes during the nucleation of gas hydrates (54), subsequently delaying the formation of initial gas hydrate agglomerates. This delay is part of an accumulative process concerning the potential energy involved in the agglomeration of crystalline hydrates. Paraffin, by postponing the formation of hydrate crystals, contributes to the sudden formation of large agglomerates when its role as a kinetic inhibitor of hydrate formation becomes overwhelmed (55).

The main factors that promote the formation of crystalline hydrates in the reactor are the super cooling of the system and the super saturation of the system with free gas. The super cooling aspect precisely defines the thermobaric conditions favorable for the nucleation process of gas hydrates. The kinetics of hydrate formation is greatly dependent on the level of super saturation. To accelerate the formation of gas hydrate deposits within the reactor, it is simply necessary to enhance the degree of gas super saturation in the system

by increasing the stirring speed. However, for the purpose of this experiment, the degree of super cooling and super saturation of the system is to be kept constant.

Accordingly, to investigate the effect of paraffin on the nucleation rate and kinetic characteristics of gas hydrate formation, the following methodology was developed. The process of nucleation and formation of crystalline hydrates is recognized as a relatively stochastic process, which introduces additional challenges in the investigation of this phenomenon (56). The variability in the time intervals for the formation of hydrate agglomerates necessitates the identification of dissociation conditions when determining the equilibrium point. Hydrate dissociation consistently occurs at a uniform rate, reaching equilibrium conditions simultaneously. However, this approach does not specifically cater to the study of the nucleation rate of hydrate crystals. Thus, the methodology proposed herein aims to evaluate the impact of varying concentrations of paraffin in the system on the nucleation rate of gas hydrate crystals.

The methodology for this laboratory experiment is outlined as follows:

1. Preparation of Paraffin Solution in Kerosene:

- The procedure for preparing the paraffin solution is identical to that described in section 2.2.

2. Preparation of the Autoclave for the Experiment:

- This step is conducted in the same manner as the autoclave preparation outlined in section 2.2.

3. Experiment on Determining the Nucleation Time of Gas Hydrates:

- To ensure the emulsion's stability and maintain a constant degree of system super saturation, the stirrer speed is set at 200 rpm. This speed is maintained uniformly throughout the experiment.
- Utilizing previously identified equilibrium points of hydrate formation, the intervals for system cooling are determined. The reactor is set to the required system pressure. Subsequently, the liquids and gas within the reactor are cooled from a starting temperature of 22°C to a temperature that is 1°C higher than the hydrate formation temperature over a period of 1.5 hours.
- The system is then further cooled to a temperature 2-3°C below the hydrate formation temperature, based on the specific conditions required. This cooling phase lasts for 30 minutes, after which the system is poised for the holding phase of the experiment.
- The system is maintained under these conditions for 10 hours (although this duration may be adjusted based on empirical observations), during which the pressure and temperature within the system, as well as the torque exerted by the stirrer, are meticulously recorded.
- Throughout the nucleation phase, the system's pressure and temperature are kept constant. Upon reaching the equilibrium conditions, the hydrate formation process initiates, characterized by a reduction in pressure as the gas transitions into the hydrate molecules, and a notable increase in temperature due to the exothermic nature of hydrate agglomerate formation.
- The duration from the start of the experiment to the nucleation and formation of hydrates is accurately documented. Following this, the autoclave is reheated to room temperature, and the experiment is restarted. This repetition is crucial for reducing the stochastic variability inherent in the formation of gas hydrates. Initially, it is planned to conduct 10 experiments at a single paraffin mass content to calculate the average time required for the nucleation of crystalline hydrates.

3. RESULTS AND DISCUSSION

From these investigations, several key insights were uncovered. Primarily, a methodology for determining the depth of crystalline hydrates and Asphaltene Resin Paraffin Deposits (ARPD) formation within a producing well was introduced. This algorithm facilitates the precise identification of the depth at which organic deposits form, contingent on specific operational parameters of well equipment. Moreover, there exists potential to refine this method by integrating new relationships and differential equations. These equations would account for the gas hydrates' nucleation time in the presence of paraffin within the flow, deriving their foundation from the laboratory studies executed in this research.

Secondly, the acquisition of the equilibrium hydrate formation curve, illustrated in Figure 9, was for a system containing a 5% paraffin content. Additionally, data points for a 2% paraffin content, with all other parameters of the gas-liquid system and the autoclave remaining constant, were also derived. It was determined that paraffin does not influence the thermobaric conditions necessary for the formation of crystalline hydrates.

Thirdly, patterns regarding the nucleation time of hydrate crystals in systems containing paraffin were identified. The impact of paraffin on the nucleation time was specifically assessed for systems with 2 and 5% mass content of paraffin solution in kerosene, revealing nuanced insights into how paraffin presence affects the initial stages of hydrate crystal formation.

Several hypotheses were corroborated through the study, leading to the identification of distinct patterns:

- The nucleation process and the formation of crystalline hydrates exhibit a stochastic nature, with the time required ranging from 30 minutes to several hours, as illustrated in Figures 10 and 11.
- The modeling compound demonstrates a memory effect (57), wherein successive experiments yield nearly identical nucleation times. This memory

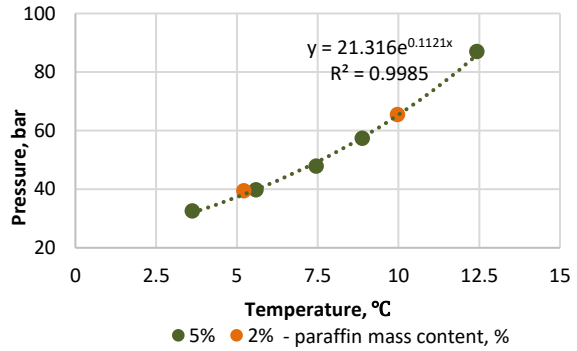

Figure 9. Equilibrium curve of hydrate formation obtained during the experiment

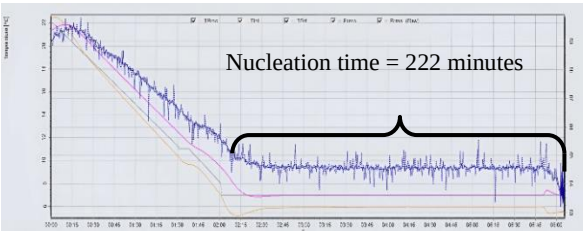

Figure 10. Equilibrium curve of hydrate formation obtained during the experiment

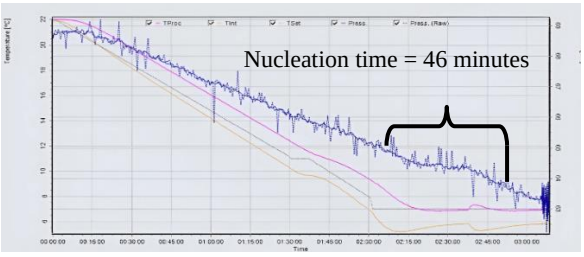

Figure 11. Hydrate nucleation less than one hour

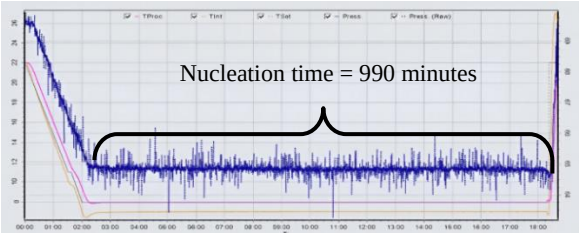

Figure 12. Equilibrium curve of hydrate formation obtained during the experiment

effect also facilitates the accelerated formation of gas hydrates in subsequent experiments, highlighting an intriguing aspect of the compound's behavior under experimental conditions.

- The degree of super cooling has a significant impact on the nucleation time. Decreasing the super cooling temperature from 3 to 2°C led to a fivefold increase in nucleation time, as depicted in Figure 12.
- The presence of wax in the mixture markedly prolongs the nucleation time of gas hydrates. With a 2% wax mass content, the average nucleation time was recorded at 94 minutes, whereas for a wax content of 5%, the nucleation time extended to 826 minutes. This represents a nine-fold increase in average nucleation time. Such variations underscore the role of increased wax content in impeding mass and heat transfer among hydrate molecules; thus inhibiting the formation of sizable gas hydrate agglomerates. This discovery underscores the importance of considering the inhibitory effects of wax on the formation of gas hydrate deposits during oil extraction processes. The outcomes of these investigations are summarized in Tables 1 and 2.

The variability observed in Tables 1 and 2 may be attributed to both the stochastic nature of the nucleation process and the memory effect. Specifically, the water molecules' hydrogen bonds surrounding the guest gas molecule, following hydrate decomposition, are preserved. Upon subsequent cooling, these bonds more readily serve as crystallization nuclei, thereby shortening the induction period (58).

To rigorously assess the impact of paraffin, a null hypothesis was posited prior to experimentation: "The hydrate nucleation time for a mixture with 2% wax mass content is equivalent to that for a mixture with 5% wax mass content," with a p-value threshold set at 0.05. This hypothesis was examined utilizing the SciPy library within the Python programming language.

The null hypothesis was ultimately refuted, as the statistical analysis yielded a p-value of 0.035, against the preset threshold of 0.05. This outcome indicates a significant difference in the hydrate nucleation times between mixtures with 2 and 5% wax mass content. Consequently, it is inferred that paraffin acts as a natural kinetic inhibitor in the formation of gas hydrates, highlighting its potential utility in managing gas hydrate formation in oil production contexts.

TABLE 1. Results of 10 experiments with 2% paraffin

Hydrates nucleation time	Experiment number									
	1	2	3	4	5	6	7	8	9	10
From equilibrium conditions of hydrate formation, min	222	240	32	43	46	35	19	19	239	40

TABLE 2. Results of 10 experiments with 5% paraffin

Hydrates nucleation time	Experiment number									
	1	2	3	4	5	6	7	8	9	10
From equilibrium conditions of hydrate formation, min	53	240	57	148	2645	1945	27	540	440	2160

4. CONCLUSION

The research delineated in this manuscript pertains to the elucidation of conditions conducive to the simultaneous formation of gas hydrates and asphaltene-resin-paraffin deposits (ARPD) within wellbores. The authors have developed a comprehensive methodology encompassing an extensive range of calculations. This methodology initiates with the determination of the thermobaric conditions prevailing inside the wellbore and culminates in the analysis of equilibrium conditions pertinent to hydrate formation alongside the crystallization temperature of paraffin. This study meticulously considers vital aspects of the reservoir fluid production process, including gas saturation, the distribution and dispersion of free gas within the flow, oil shrinkage, the presence of free water, and the impact of fluid viscosity on the operational parameters of Electric Submersible Pumps (ESP). This approach ensures a holistic understanding of the phenomena under study, integrating crucial factors that influence the formation of these deposits.

The computational algorithm introduced in this article holds promise for enhancing hydrocarbon production methodologies. Additionally, there is scope for the refinement and modernization of this algorithm to better meet the evolving needs of the industry.

During the course of laboratory experiments, it was ascertained that paraffin plays a significant role in influencing the kinetic conditions pertinent to the nucleation of gas hydrates. Notwithstanding, evidence suggests that paraffin embedded within kerosene does not alter the thermobaric conditions requisite for the formation of gas hydrates. Thus, paraffin emerges as a natural kinetic inhibitor, given that the nucleation rate of hydrates at a designated super cooling temperature escalates with an increase in its concentration within kerosene. Consequently, incorporating the nucleation timing in the context of wax presence facilitates the formulation of a temporal operational model for wells. This model, predicated on differential equations, juxtaposes the duration of fluid evacuation from the wellbore against the formation timeline of gas hydrate deposits. The implementation of this model is aimed at establishing operational conditions within the wellbore that preempt the formation of gas hydrates, particularly in regions where combating their accumulation proves most challenging.

Future experimental endeavors aimed at pinpointing the most likely nucleation interval for hydrate formation necessitate a methodological recalibration to mitigate the 'memory effect' observed during the reformation of gas hydrates. Within the ambit of this study, experiments demonstrated a prolongation in nucleation timing when the mixture was preheated to 35-40°C before subsequent re-cooling. It is noteworthy that the memory effect could be contingent upon the provenance of the water and its dwell time subsequent to hydrate dissociation.

The insights garnered from this research elucidate the formation mechanisms of crystalline hydrates and paraffin deposits, paving the way for the innovation of more efficacious strategies to thwart their accumulation in oil wells. This advancement harbors the potential to improve efficiency, curtail maintenance and operational expenditures, and engender more consistent production outcomes for oil entities.

5. REFERENCES

1. Mastronardo E, La Mazza E, Palamara D, Piperopoulos E, Iannazzo D, Proverbio E, et al. Organic salt hydrate as a novel paradigm for thermal energy storage. Energies. 2022;15(12):4339. https://doi.org/10.3390/en15124339
2. Zhang J, Li C, Shi L, Xia X, Yang F, Sun G. The formation and aggregation of hydrate in W/O emulsion containing different compositions: A review. Chemical Engineering Journal. 2022;445:136800. https://doi.org/10.1016/j.cej.2022.136800
3. Semenov AP, Stoporev AS, Mendgaziev RI, Gushchin PA, Khlebnikov VN, Yakushev VS, et al. Synergistic effect of salts and methanol in thermodynamic inhibition of sII gas hydrates. The Journal of Chemical Thermodynamics. 2019;137:119-30. https://doi.org/10.1016/j.jct.2019.05.013
4. Borisova NN, Rozhin II. Method for determining the mass flow for pressure measurements of gas hydrates formation in the well. Журнал Сибирского федерального университета Серия «Математика и физика». 2021;14(2):193-203. https://doi.org/10.17516/1997-1397-2021-14-2-193-203
5. Raupov I, Burkhanov R, Lutfullin A, Maksyutin A, Lebedev A, Safiullina E. Experience in the application of hydrocarbon optical studies in oil field development. Energies. 2022;15(10):3626. https://doi.org/10.3390/en15103626
6. Nikolaichuk L, Ignatiev K, Filatova I, Shabalova A. Diversification of Portfolio of International Oil and Gas Assets using Cluster Analysis. International Journal of Engineering, Transactions A: Basics. 2023;36(10):1783-92. https://doi.org/10.5829/IJE.2023.36.10A.06
7. Tananykhin D, Struchkov I, Khormali A, Roschin P. Investigation of the influences of asphaltene deposition on oilfield development using reservoir simulation. Petroleum Exploration

and Development. 2022;49(5):1138-49. https://doi.org/10.1016/S1876-3804(22)60338-0

8. Duryagin V, Nguyen Van T, Onegov N, Shamsutdinova G. Investigation of the selectivity of the water shutoff technology. Energies. 2022;16(1):366. https://doi.org/10.3390/en16010366
9. Raupov I, Rogachev M, Sytnik J. Design of a polymer composition for the conformance control in heterogeneous reservoirs. Energies. 2023;16(1):515. https://doi.org/10.3390/en16010515
10. Cherepovitsyn AE, Tsvetkov PS, Evseeva OO. Critical analysis of methodological approaches to assessing sustainability of arctic oil and gas projects. Записки Горного института. 2021;249:463-78. https://doi.org/10.31897/PMI.2021.3.15
11. Litvinenko VS, Tsvetkov PS, Dvoynikov MV, Buslaev GV. Barriers to implementation of hydrogen initiatives in the context of global energy sustainable development. Записки Горного Института. 2020;244:428-38. https://doi.org/10.31897/PMI.2020.4.5
12. Van TN, Aleksandrov AN, Rogachev MK. An extensive solution to prevent wax deposition formation in gas-lift wells. Journal of Applied Engineering Science. 2022;20(1):264-75. https://doi.org/10.1007/s13202-022-01598-8
13. Nguyen VT, Pham TV, Rogachev MK, Korobov GY, Parfenov DV, Zhurkevich AO, et al. A comprehensive method for determining the dewaxing interval period in gas lift wells. Journal of Petroleum Exploration and Production Technology. 2023;13(4):1163-79.
14. Martins JR, da Cunha Ribeiro D, Pereira FdAR, Ribeiro MP, Romero OJ. Heat dissipation of the Electrical Submersible Pump (ESP) installed in a subsea skid. Oil & Gas Science and Technology–Revue d'IFP Energies nouvelles. 2020;75:13. https://doi.org/10.2516/ogst/2020009
15. Manabe R, Wang Q, Zhang H-Q, Sarica C, Brill JP, editors. A mechanistic heat transfer model for vertical two-phase flow. SPE Annual Technical Conference and Exhibition?; 2003: SPE.
16. Gao Y, Cui Y, Xu B, Sun B, Zhao X, Li H, et al. Two phase flow heat transfer analysis at different flow patterns in the wellbore. Applied thermal engineering. 2017;117:544-52. https://doi.org/10.1016/j.applthermaleng.2017.02.058
17. Serbin DV, Dmitriev AN. Experimental research on the thermal method of drilling by melting the well in ice mass with simultaneous controlled expansion of its diameter. Записки Горного института. 2022;257:833-42. https://doi.org/10.31897/PMI.2022.82
18. Wang X, Wang Z, Deng X, Sun B, Zhao Y, Fu W. Coupled thermal model of wellbore and permafrost in Arctic regions. Applied Thermal Engineering. 2017;123:1291-9. https://doi.org/10.1016/j.applthermaleng.2017.05.186
19. Merey S, Aydin H, Eren T. Design of electrical submersible pumps in methane hydrate production wells: A case study in Nankai trough methane hydrates. Upstream Oil and Gas Technology. 2020;5:100023. https://doi.org/10.1016/j.upstre.2020.100023
20. Mardashov DV, Bondarenko AV, Raupov IR. Technique for calculating technological parameters of non-Newtonian liquids injection into oil well during workover. Записки Горного института. 2022;258:881-94. https://doi.org/10.31897/pmi.2022.16
21. Mardashov DV. Development of blocking compositions with a bridging agent for oil well killing in conditions of abnormally low formation pressure and carbonate reservoir rocks. Записки Горного института. 2021;251:667-77. https://doi.org/10.31897/pmi.2021.5.6
22. Fu W, Wang Z, Sun B, Ji C, Zhang J. Multiple controlling factors for methane hydrate formation in water-continuous system. International Journal of Heat and Mass Transfer. 2019;131:757-71. https://doi.org/10.1016/j.ijheatmasstransfer.2018.10.025
23. Aman ZM, Di Lorenzo M, Kozielski K, Koh CA, Warrier P, Johns ML, et al. Hydrate formation and deposition in a gas-dominant flowloop: Initial studies of the effect of velocity and subcooling. Journal of Natural Gas Science and Engineering. 2016;35:1490-8. https://doi.org/10.1016/j.jngse.2016.05.015
24. Zhou S, Chen X, He C, Wang S, Zhao S, Lv X. Experimental study on hydrate formation and flow characteristics with high water cuts. Energies. 2018;11(10):2610. https://doi.org/10.3390/en11100000
25. Guimin Y, Hao J, Qingwen K. Study on hydrate risk in the water drainage pipeline for offshore natural gas hydrate pilot production. Frontiers in Earth Science. 2022;9:816873. https://doi.org/10.3389/feart.2021.816873
26. Kuzmin AM, Buslaev GV, Morenov VA, Tseneva SN, Gavrilov NA. Improving the energy-efficiency of small-scale methanol production through the use of microturboexpander units. Записки Горного института. 2022;258:1026-37. https://doi.org/10.31897/PMI.2022.104
27. Ilyushin P, Vyatkin K, Kozlov A. Development of a method for estimating thermal conductivity of organic deposits on the wax flow loop laboratory installation. International Journal of Engineering, Transactions C: Aspects 2022;35(6):1178-85. https://doi.org/10.5829/IJE.2022.35.06C.09
28. Rogachev MK, Aleksandrov AN. Justification of a comprehensive technology for preventing the formation of asphalt-resin-paraffin deposits during the production of highly paraffinic oil by electric submersible pumps from multiformation deposits. Записки Горного института. 2021;250:596-605. https://doi.org/10.31897/PMI.2021.4.13
29. Petrakov D, Loseva A, Alikhanov N, Jafarpour H. Standards for selection of surfactant compositions used in completion and stimulation fluids. International Journal of Engineering, Transactions C: Aspects 2023;36(9):1605-10. https://doi.org/10.5829/IJE.2023.36.09C.03
30. Khaibullina KS, Sagirova LR, Sandyga MS. Substantiation and selection of an inhibitor for preventing the formation of asphalt-resin-paraffin deposits. Periodico Tche Quimica. 2020;17(34). https://doi.org/10.52571/ptq.v17.n34.2020.565_p34_pgs_541_551.pdf
31. Nurgalieva KS, Saychenko LA, Riazi M. Improving the efficiency of oil and gas wells complicated by the formation of Asphalt–Resin–Paraffin deposits. Energies. 2021;14(20):6673. https://doi.org/10.3390/en14206673
32. Бельский А, Моренов В, Купавых К, Сандыга М. Электроснабжение станции нагрева нефти в скважине от ветроэлектрической установки. Энергетика Известия высших учебных заведений и энергетических объединений СНГ. 2019;62(2):146-54. https://doi.org/10.21122/1029-7448-2019-62-2-146-154
33. Li R, Huang Q, Zhu X, Zhang D, Lv Y, Larson RG. Investigation of delayed formation of wax deposits in polyethylene pipe using a flow-loop. Journal of Petroleum Science and Engineering. 2021;196:108104. https://doi.org/10.1016/j.petrol.2020.108104
34. Юдин П, Богатов М. Моделирование процесса выпадения асфальтосмолопарафиновых веществ на внутренней поверхности насосно-компрессорных труб с покрытием и без на лабораторном циркуляционном стенде. Нефтегазовое дело. 2021;19(2):97-103. https://doi.org/10.17122/ngdelo-2021-2-97-103
35. Bai J, Jin X, Wu J-T. Multifunctional anti-wax coatings for paraffin control in oil pipelines. Petroleum Science. 2019;16(3):619-31. https://doi.org/10.1007/s12182-019-0309-7
36. Kovrigin L, Kukharchuk I. Automatic control system for removal of paraffin deposits in oil well in permafrost region by thermal

method. Chemical Engineering Research and Design. 2016;115:116-21. https://doi.org/10.1016/j.cherd.2016.09.028

37. Голубев И, Голубев А, Лаптев А. Практика применения аппаратов магнитной обработки для интенсификации процессов первичной подготовки нефти. Записки Горного института. 2020;245:554-60. https://doi.org/10.31897/PMI.2020.5.7
38. Sizikov AA, Vlasov VA, Stoporev AS, Manakov AY. Decomposition kinetics and self-preservation of methane hydrate particles in crude oil dispersions: experiments and theory. Energy & fuels. 2019;33(12):12353-65. https://doi.org/10.1021/acs.energyfuels.9b03391
39. Stoporev AS, Manakov AY, Altunina LK, Bogoslovsky AV, Strelets LA, Aladko EY. Unusual self-preservation of methane hydrate in oil suspensions. Energy & fuels. 2014;28(2):794-802. https://doi.org/10.1021/ef401779d
40. Wang W, Huang Q, Zheng H, Wang Q, Zhang D, Cheng X, et al. Effect of wax on hydrate formation in water-in-oil emulsions. Journal of Dispersion Science and Technology. 2020;41(12):1821-30. https://doi.org/10.1080/01932691.2019.1637751
41. Liu Y, Meng J, Lv X, Ma Q, Shi B, Wang C, et al. Investigating hydrate formation and flow properties in water-oil flow systems in the presence of wax. Frontiers in Energy Research. 2022;10:986901. https://doi.org/10.3389/fenrg.2022.986901
42. Zi M, Wu G, Wang J, Chen D. Investigation of gas hydrate formation and inhibition in oil-water system containing model asphaltene. Chemical Engineering Journal. 2021;412:128452. https://doi.org/10.1016/j.cej.2021.128452
43. Hang J, Bai L, Zhou L, Jiang L, Shi W, Agarwal R. Inter-stage energy characteristics of electrical submersible pump under gassy conditions. Energy. 2022;256:124624. https://doi.org/10.1016/j.energy.2022.124624
44. Bulgarelli NAV, Biazussi JL, Verde WM, Perles CE, de Castro MS, Bannwart AC. Experimental investigation of the electrical submersible pump's energy consumption under unstable and stable oil/water emulsions: A catastrophic phase inversion analysis. Journal of Petroleum Science and Engineering. 2022;216:110814. https://doi.org/10.1016/j.petrol.2022.110814
45. Zhou L, Hang J, Bai L, Krzemianowski Z, El-Emam MA, Yasser E, et al. Application of entropy production theory for energy losses and other investigation in pumps and turbines: A review. Applied Energy. 2022;318:119211. https://doi.org/10.1016/j.apenergy.2022.119211
46. Zhang M, Jia A, Lei Z, Lei G. A Comprehensive Asset Evaluation Method for Oil and Gas Projects. Processes. 2023;11(8):2398. https://doi.org/10.3390/pr11082398
47. Tomescu SG, Mălăel I, Conțiu R, Voicu S. Experimental Validation of the Numerical Model for Oil–Gas Separation. Inventions. 2023;8(5):125. https://doi.org/10.3390/inventions8050125
48. Arzhanov MM, Malakhova VV, Mokhov II. Modeling thermal regime and evolution of the methane hydrate stability zone of the Yamal peninsula permafrost. Permafrost and Periglacial Processes. 2020;31(4):487-96. https://doi.org/10.1002/ppp.2074
49. Yakushev V, Semenov A, Bogoyavlensky V, Medvedev V, Bogoyavlensky I. Experimental modeling of methane release from intrapermafrost relic gas hydrates when sediment temperature change. Cold Regions Science and Technology. 2018;149:46-50. https://doi.org/10.1016/j.coldregions.2018.02.007
50. Semenov A, Mendgaziev R, Stoporev A, Istomin V, Tulegenov T, Yarakhmedov M, et al. Direct Measurement of the Four-Phase Equilibrium Coexistence Vapor–Aqueous Solution–Ice–Gas Hydrate in Water–Carbon Dioxide System. International Journal of Molecular Sciences. 2023;24(11):9321. https://doi.org/10.3390/ijms24119321
51. Lekomtsev A, Kozlov A, Kang W, Dengaev A. Designing of a washing composition model to conduct the hot flushing wells producing paraffin crude oil. Journal of Petroleum Science and Engineering. 2022;217:110923. https://doi.org/10.1016/j.petrol.2022.110923
52. Liu Y, Wu C, Lv X, Xu X, Ma Q, Meng J, et al. Evolution of morphology and cohesive force of hydrate particles in the presence/absence of wax. RSC advances. 2022;12(23):14456-66. https://doi.org/10.1039/D2RA02266D
53. Semenov AP, Medvedev VI, Gushchin PA, Yakushev VS. Effect of heating rate on the accuracy of measuring equilibrium conditions for methane and argon hydrates. Chemical Engineering Science. 2015;137:161-9. https://doi.org/10.1016/j.ces.2015.06.031
54. Liu Y, Wu C, Lv X, Du H, Ma Q, Wang C, et al. Hydrate growth and agglomeration in the presence of wax and anti-agglomerant: A morphology study and cohesive force measurement. Fuel. 2023;342:127782. https://doi.org/10.1016/j.fuel.2023.127782
55. Tong S, Li P, Lv F, Wang Z, Fu W, Zhang J, et al. Promotion and inhibition effects of wax on methane hydrate formation and dissociation in water-in-oil emulsions. Fuel. 2023;337:127211. https://doi.org/10.1016/j.fuel.2022.127211
56. Liu Z, Wang Z, Chen L, Chen L, Li X, Sun B. Experimental and modeling investigations of hydrate phase equilibria in natural clayey-silty sediments. Chemical Engineering Journal. 2022;449:137557. https://doi.org/10.1016/j.cej.2022.137557
57. Gao Q, Zhao J, Guan J, Zhang C. Influence of the memory effect during CO2/CH4 mixed gas hydrate reformation process. Fuel. 2023;353:129249. https://doi.org/10.1016/j.fuel.2023.129249
58. Wen Z, Yao Y, Luo W, Lei X. Memory effect of CO2-hydrate formation in porous media. Fuel. 2021;299:120922. https://doi.org/10.1016/j.fuel.2021.120922

Persian Abstract

چکیده

هدف از این کار آنالیز زمان هسته زایی مولکول های هیدرات گاز در جریان نفت است .این تحقیق با هدف بررسی تأثیر ذرات پارافین بر زمان تشکیل رسوبات هیدرات در طی تولید مکانیزه نفت انجام شده است .درک و مدیریت صحیح تشکیل رسوبات آلی در فضای چاه می تواند هزینه های نگهداری تجهیزات را به میزان قابل توجهی کاهش دهد، ایمنی و پایداری تولید را افزایش دهد و بازده اقتصادی تولید هیدروکربن را بهبود بخشد .بخش اول مقاله روشی برای تعیین عمق تشکیل هیدرات های گازی و رسوبات آسفالت-رزین-پارافین (ARPD) در تولید چاه های نفت با حل سیستم های معادلات دیفرانسیل ترموباریک ارائه می کند .مطالعات آزمایشگاهی بیشتری برای تجزیه و تحلیل زمان هسته زایی هیدرات های گازی در حضور پارافین انجام شد .این آزمایش در یک اتوکلاو فشار بالا ویژه انجام شد که در آن امکان ایجاد شرایط ترموباریک لازم وجود دارد .همزن داخل اتوکلاو پراکندگی لازم سیستم را برای شبیه سازی جریان در چاه ایجاد می کند .در نتیجه آزمایش ها مشخص شد که ذرات پارافین مانع از تشکیل رسوبات هیدرات گاز شده و روند هسته زایی آنها را کند می کند .همچنین مشخص شد که افزایش محتوای پارافین در مخلوط به میزان 3 درصد، زمان هسته زایی هیدرات های گازی را 9 برابر افزایش می دهد .بر اساس تجزیه و تحلیل داده های موجود، نتیجه گیری می شود که برای توسعه مدل زمانی عملیات چاه تولیدی تحت شرایط هیدرات گاز و تشکیل ARPD به مطالعات عمیق تری نیاز است.